# Alternating Zinc Fingers in the Human Male-Associated Protein ZFY: $HX_3H$ and $HX_4H$ Motifs Encode a Local Structural Switch[†,‡]

Michel Kochoyan,[§,∥] Henry T. Keutmann,[⊥] and Michael A. Weiss[*,§,⊥]

*Department of Biological Chemistry and Molecular Pharmacology, Harvard Medical School, Boston, Massachusetts 02115, and Department of Medicine, Massachusetts General Hospital, Boston, Massachusetts 02114*

*Received May 15, 1991; Revised Manuscript Received July 24, 1991*

ABSTRACT: The two-finger repeat in the human male-associated protein ZFY provides a model for comparative 2D-NMR studies of classical and variant Zn fingers. This repeat is defined in part by an alternation in spacing between consensus ($HX_3H$) and variant ($HX_4H$) histidine spacings. To investigate the effects of a "switch" between alternative histidine spacings, we have designed an $HX_3H$ analogue of a representative $HX_4H$ domain of known structure [ZFY-6; Kochoyan, M., Havel, T., Nguyen, D. T., Dahl, C. E., Keutmann, H. T., & Weiss, M. A. (1991) *Biochemistry 30*, 3371–3386]. The $HX_3H$ analogue (designated ZFY-switch) forms a tetrahedral $Co^{2+}$ complex whose thermodynamic stability is similar to that of the parent peptide. 2D-NMR studies demonstrate that ZFY-switch and ZFY-6, although similar in overall structure, exhibit significant local changes near the site of deletion. Whereas the $HX_4H$ site in the native finger forms a nonstandard loop, the $HX_3H$ site in ZFY-switch folds as a $3_{10}$ extension of the C-terminal $\alpha$-helix, as observed in the NMR solution structure of a consensus $HX_3H$ domain [Lee, M. S., Gippert, G. P., Soman, K. V., Case, D. A., & Wright, P. E. (1989) *Science 245*, 635–637] and in the crystal structure of a representative Zn finger–DNA complex [Pavletich, N. P., & Pabo, C. O. (1991) *Science 252*, 809–817]. We propose that variant histidine spacings ($HX_3H$ and $HX_4H$) encode a local switch between alternative surface architectures with implications for models of protein–DNA recognition.

ZFY, a putative human transcription factor encoded by the sex-determining region of the Y chromosome (Page et al., 1987), is proposed to participate in spermatogenesis (Palmer et al., 1989; Koopman et al., 1989) and in the regulation of male embryogenesis (Page et al., 1990). The sequence of ZFY contains a two-finger repeat, which is conserved within a vertebrate gene family (DiLella et al., 1990). Whereas the odd-numbered domains are similar to the general Zn finger consensus (Klug & Rhodes, 1986; Gibson et al., 1988), the even-numbered domains exhibit systematic differences. This repeat provides a model for alternative Zn finger templates (Weiss et al., 1990) whose structural implications may be investigated by comparative studies of finger analogues (Weiss & Keutmann, 1990). The solution structure of a representative even-numbered domain (ZFY-6;[1] Kochoyan et al., 1991a,b) has recently been shown to share the classical $\beta\beta\alpha$ structure (Gibson et al., 1987; Berg, 1987) observed in consensus Zn fingers (Parraga et al., 1988; Lee et al., 1989; Klevit et al., 1990; Omichinski et al., 1990).

In this paper we investigate the structural implications of one aspect of the ZFY two-finger repeat, alternation in spacing between histidines involved in $Zn^{2+}$ coordination: $HX_3H$ in odd-numbered domains and $HX_4H$ in even-numbered domains (DiLella et al., 1990). Such alternation has also been observed in an extensive collection of Zn finger sequences in *Xenopus laevis* (Nietfeld et al., 1989), and related alternation between $HX_3H$- and $HX_5H$-containing domains is observed in a human enhancer-binding protein (Maekawa et al., 1989; Fan & Maniatis, 1990; Baldwin et al., 1990). The role of alternative ligand spacing in DNA recognition is not understood. Unlike $HX_3H$ Zn fingers, which frequently are observed in multiple repeats (Gibson et al., 1987), contiguous $HX_4H$ or $HX_5H$ sequences are rare. A model in which alternating $HX_4H$ linker units span the minor groove has recently been proposed (the "jumping linker" model; Kochoyan et al., 1991a).

2D-NMR structures of representative Zn fingers containing $HX_3H$ (Lee et al., 1989; Klevit et al., 1990), $HX_4H$ (Kochoyan et al., 1991a,b), and $HX_5H$ (Omichinski et al., 1990) spacings each exhibit an N-terminal $\beta$-sheet and C-terminal $\alpha$-helix ($\beta\beta\alpha$ motif), as predicted by model building (Gibson et al., 1988; Berg, 1988). Comparison of these structures suggests that variant histidine spacings encode local structural features whose configurations are essentially independent of the folding of the rest of the domain. In addition to $HX_{3-5}H$ variation, however, the peptides studied to date contain multiple sequence substitutions, thus complicating straightforward interpretation of structural differences. To investigate the implications of changes in ligand spacing *in an otherwise identical sequence*

[†] Supported by the Lucille Markey Charitable Trust and by grants from the National Institutes of Health, American Cancer Society, and the Pfizer Scholars Program for New Faculty and by a Junior Faculty Research Award from the American Cancer Society. M.K. is supported in part by a "Fondation Pour La Recherche Medicale" postdoctoral fellowship.

[‡] The coordinates of the NMR structures and table of NMR-based restraints have been deposited in the Brookhaven Protein Data Bank.

[*] Address correspondence to this author at the Department of Biological Chemistry and Molecular Pharmacology at Harvard Medical School.

[§] Harvard Medical School.

[∥] Permanent address: CNRS URA 32, Biop Polytechnique, 91128 Palaiseau, France.

[⊥] Massachusetts General Hospital.

[1] Abbreviations: DQF-COSY, double-quantum-filtered correlated spectroscopy; DG, distance geometry; NMR, nuclear magnetic resonance; NOESY, nuclear Overhauser effect spectroscopy; RMD, restrained molecular dynamics; rms, root mean square; SA, simulated annealing; TOCSY, total correlation spectroscopy; ZFY-6, single Zn finger (sequence KTYQCQYCEYASADSSNLKTHIKTKHSKEK) derived from finger 6 in the human gene ZFY [exon residues 162–191 in Page et al. (1987)].

0006-2960/91/0430-9396$02.50/0 

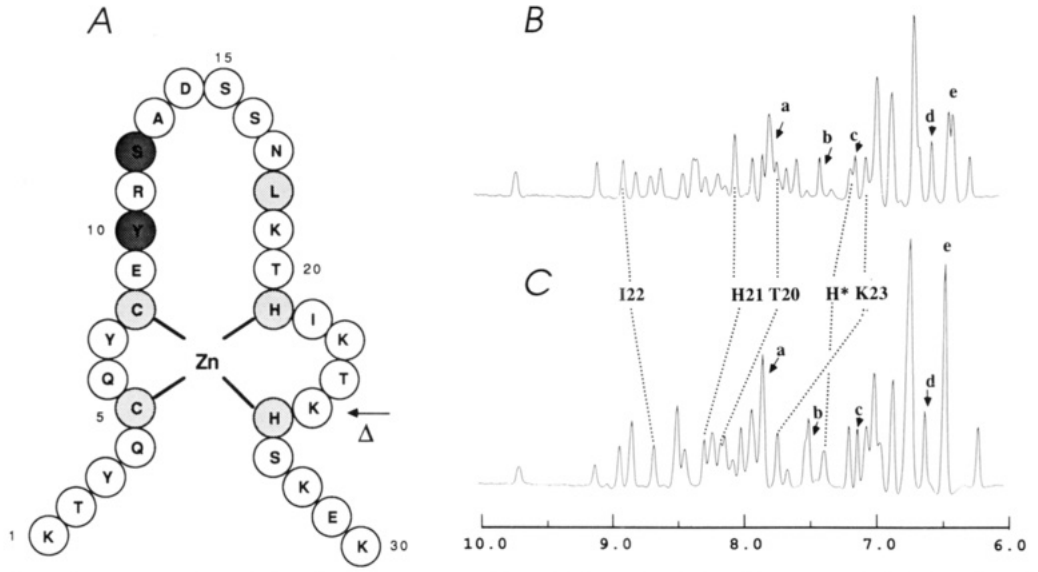


FIGURE 1: (A) Schematic representation of the primary structures of ZFY-6 (inner circles) and ZFY-switch (deletion of residue 25; indicated by Δ and arrow). Residues involved in metal binding (C5, C8, H21, and H26) and conserved "framework" leucine (L18) are lightly shaded; sites of alternative aromatic placement (Y10 and S12; Weiss & Keutmann, 1990) are heavily shaded. (B) Amide and aromatic region of 1D $^1$H NMR spectra of ZFY-switch as reduced 1:1 $Zn^{2+}$ complex in $H_2O$. (C) Corresponding spectrum of ZFY-6. In panels B and C, dashed lines connect resonances that exhibit significant changes in chemical shift (Table II). Other labeled resonances are as follows: (a) H26 $H_\epsilon$, (b) H21 $H_\epsilon$, (c) H21 $H_\delta$, (d) H25 (in ZFY-6, H26) $H_\delta$, and (e) Y10 ring resonance. The ortho and meta resonances of Y10, partially resolved in spectrum B, are degenerate in spectrum C as previously described (Kochoyan et al., 1991a,b).

*background*, we have synthesized an $HX_3H$ analogue of a representative $HX_4H$ domain (ZFY-6; Kochoyan et al., 1991a,b). This analogue (designated ZFY-switch) contains a deletion of one residue between the histidines (Figure 1A). ZFY-switch thus provides a model of a $HX_3H$ metal-binding site whose solution structure may be compared to that of the parent peptide.

## Materials and Methods

*Peptide Synthesis and Characterization.* ZFY-switch (Figure 1A) and ZFY-6 (formerly designated ZFY-6T; Kochoyan et al., 1991a) were synthesized by the solid-phase procedure, purified, and characterized as previously described (Weiss et al., 1990). The peptides were >98% pure as determined by analytical reverse-phase HPLC and sequence analysis of preview (Tregear et al., 1977).

*Visible Absorption Spectroscopy.* Metal binding of the peptide–$Co^{2+}$ complexes was evaluated by visible absorption spectroscopy from 280 to 800 nm as described (Frankel et al., 1987; Weiss et al., 1990) by using a Beckman Model 15 spectrophotometer. Spectra were obtained in 50 mM Tris-HCl buffer (pH 7.5) containing successive aliquots of $CoCl_2$. For pH titrations this buffer was mixed with aliquots of 0.1% acetic acid (containing the same concentration of $CoCl_2$ or $ZnCl_2$) to achieve intermediate pH conditions.

*NMR.* The reduced peptides (ca. 5 mM) were dissolved in 0.7 mL of NMR buffer consisting of 50 mM deuterated Tris-HCl (pH 6) and 5 mM $ZnCl_2$. Two-dimensional experiments were obtained at 500 MHz and 25 °C by the pure-phase method. Exponential and shifted sine-bell window functions were applied in both dimensions prior to Fourier transformation. *J* coupling constants were determined from analysis of high-resolution DQF-COSY spectra as previously described (Kochoyan et al., 1991a). As in the spectrum of the parent peptide, the Y10 ring resonances exhibit major (>90%) and minor (<10%) TOCSY cross peaks; only the predominant conformer is analyzed.

*NMR-Derived Restraints.* NOE and *J* coupling (dihedral angle) restraints were used for molecular modeling. (i) NOEs (mixing times 100 and 200 ms) were classified as strong (<2.7 Å), medium (<3.3 Å), or weak (<4.3 Å); the intraresidue ortho–meta cross peak of tyrosine (2.5 Å) and $H_\delta$–$H_\epsilon$ cross peak of histidine (4.3 Å) were used as internal standards. Distance-bound corrections were made for methyl groups and methylene protons for which stereospecific assignments could not be obtained (Wuthrich, 1986). (ii) Dihedral-angle restraints were introduced on the basis of *J* coupling constants. $\phi$ dihedral angles of residues with small $^3J_{HN\alpha}$ coupling constants (apparent separation <5.5 Hz) were constrained between −90° and −40°; those with large $^3J_{HN\alpha}$ coupling constants (>8.5 Hz) were constrained between −160° and −80°. Restraints were not introduced on the basis of intermediate *J* values. $\chi_1$ dihedral angles, when obtained (Table I), were restrained about the preferred rotamer with a tolerance of ±40°. A similar restraint was introduced for the $\chi_2$ dihedral angle of L18, for which stereospecific assignment of the methyl resonances was obtained in each case. Experimental restraints are provided as supplementary material.

*Structure Determination.* Distance-geometry calculations were performed with the program DG-II (T. F. Havel, Harvard Medical School). The maximum NOE restraint violation among the final DG/SA ensemble was 0.11 Å; the most consistent DG/SA structure exhibited an average NOE violation of 0.002 Å and maximum NOE violation of 0.05 Å. DG structures were subject to restrained energy minimization and restrained molecular dynamics (RMD) in vacuo by using the program XPLOR (A. T. Brunger, Yale University) by the method of Clore et al. (1985). The empirical energy function is as described by the CHARMm program (Brooks et al., 1983), and modified to include experimental and $Zn^{2+}$ coordination restraints as described (Kochoyan et al., 1991a). To avoid aberrant salt-bridge formation, the side chains of arginine, lysine, aspartic acid, and glutamic acid were assumed to be uncharged; for other electrostatic terms a dielectric constant of 80 was assumed. The maximum NOE restraint violation among the RMD ensemble was 0.12 Å; the most consistent RMD structure exhibited an average NOE violation of 0.003 Å and maximum NOE violation of 0.06 Å. Statistical pa-

Table I: Chemical Shifts of the Assigned $^1H$ NMR Resonances of ZFY-switch at pH 6.0 amd 25 °C

| | chemical shifts at 25 °C | | | |
|---|---|---|---|---|
| residue | NH | $C_\alpha H$ | $C_\beta H$ | others |
| 1 K | | | | |
| 2 T | 8.09 | 4.12 | 3.65 | $C_\gamma H_3$ 0.83 |
| 3 Y[a] | 8.62 | 4.35 | 2.85, 2.65 | $C_{2,6}H$ 6.98; $C_{3,5}$ 6.69 |
| 4 Q | 8.38 | 4.63 | 1.72, 1.80 | $C_\gamma H_2$ 2.30, 2.02 |
| 5 C[a] | 8.73 | 4.08 | 3.35, 2.70 | |
| 6 Q | 8.54 | 4.10 | 1.50, 1.50 | $C_\gamma H_2$ 1.65, 1.75 |
| 7 Y[a] | 9.66 | 4.42 | 2.40, 1.32 | $C_{2,6}H$ 6.84; $C_{3,5}$ 6.69 |
| 8 C[a] | 7.75 | 4.84 | 3.25, 3.05 | |
| 9 E | 8.28 | 4.15 | 1.88, 2.04 | $C_\gamma H_2$ 2.13 |
| 10 Y[a] | 9.03 | 3.80 | 2.51, 1.93 | $C_{2,6}H$ 6.42; $C_{3,5}$ 6.38 |
| 11 R | 6.92 | 4.92 | 1.40, 1.40 | $C_\gamma H_2$ 1.13, 1.48; $C_\delta H_2$ 3.00 |
| 12 S[a] | 8.31 | 4.33 | 3.78, 3.28 | |
| 13 A | 8.57 | 4.79 | 1.30 | |
| 14 D[a] | 8.21 | 4.79 | 2.62, 2.42 | |
| 15 S | 8.25 | 3.25 | 3.18, 3.50 | |
| 16 S | 8.31 | 4.06 | 3.85, 3.78 | |
| 17 N | 8.00 | 4.35 | 2.92, 3.00 | |
| 18 L[a] | 7.55 | 4.18 | 1.88, 1.40 | $C_\gamma H$ 1.68; $C_\delta H_3$ 0.90, 0.83 |
| 19 K | 7.85 | 3.85 | 1.80, 1.80 | $C_\gamma H_2$ 1.30; $C_\delta H_2$ 1.50; $C_\epsilon H_2$ 2.70 |
| 20 T | 7.72 | 3.75 | 4.10 | $C_\gamma H_3$ 1.10 |
| 21 H[a] | 8.00 | 3.88 | 3.12, 2.48 | $C_2H$ 7.35; $C_4H$ 6.83 |
| 22 I | 8.83 | 3.55 | 1.92 | $C_\gamma H_3$ 1.05; $C_\gamma H_2$ 1.60, $C_\delta H_3$ 1.00 |
| 23 K | 7.02 | 3.95 | 1.72, 1.72 | $C_\gamma H_2$ 1.42; $C_\delta H_2$ 1.55; $C_\epsilon H_2$ 2.80 |
| 24 T | 7.60 | 3.70 | 4.08 | $C_\gamma H_3$ 1.00 |
| 25 H | 7.12 | 4.38 | 2.60, 2.60 | $C_2H$ 7.85; $C_4H$ 6.55 |
| 26 S | 7.55 | 4.18 | 3.72, 3.72 | |
| 27 K | 8.06 | 4.18 | 1.70, 1.57 | $C_\gamma H_2$ 1.18; $C_\delta H_2$ 1.48; $C_\epsilon H_2$ 2.80 |
| 28 E | 8.12 | 4.08 | 1.75, 1.88 | $C_\gamma H_2$ 2.08 |
| 29 K | 7.73 | 3.95 | 1.55, 1.65 | $C_\gamma H_2$ 1.20; $C_\delta H_2$ 1.50; $C_\epsilon H_2$ 2.80 |

[a] $\beta$ protons stereospecifically assigned.

rameters characterizing the DG/RMD ensemble are given in Table III.

## Results

*Peptide Design and Characterization.* The even-specific $HX_4H$ sequence of ZFY-6 may in principle be changed to an odd-specific $HX_3H$ sequence by deletion of any one of the intervening residues ($H_{21}$IKTK$H_{26}$). Guided by sequence patterns conserved among odd-numbered domains (DiLella et al., 1990), we chose to delete residue $K_{25}$, creating the $HX_3H$ site $H_{21}$IKT$H_{25}$ (Figure 1). ZFY-switch thus retains a hydrophobic residue at position 22 (as in domains 1, 5, 7, 9, 11, and 13), a positively charged residue at position 23 (as in domains 1, 5, and 11), and threonine at position 24 (as in domain 11).

The visible absorption spectrum of the ZFY-switch/$Co^{2+}$ complex exhibits d–d and thiolate charge-transfer bands characteristic of tetrahedral coordination (Fraenkel et al., 1987); these are identical with those of the parent peptide (Weiss & Keutmann, 1990). The amplitude of these bands may be used to monitor pH-dependent unfolding. For ZFY-switch the midpoint of this transition (pH 5.6) is in the range of previously characterized Zn fingers (Weiss & Keutmann, 1990), indicating that this deletion mutant, unlike a previously described "fingertip" deletion in an ADR1 peptide (Parraga et al., 1990), retains a stably folded metal-binding site. The parent peptide is somewhat more stable (midpoint 5.2; Kochoyan et al., 1991a).

*NMR Studies of ZFY-switch.* In Figure 1 are shown 1D NMR spectra (amide and aromatic regions in $H_2O$) of ZFY-switch (panel B) and ZFY-6 (panel C) in the presence of equimolar $Zn^{2+}$. The two spectra exhibit similar dispersion of chemical shifts, consistent with retention of native structure in the analogue. Sequential assignment of ZFY-switch has been obtained essentially as described for the parent peptide

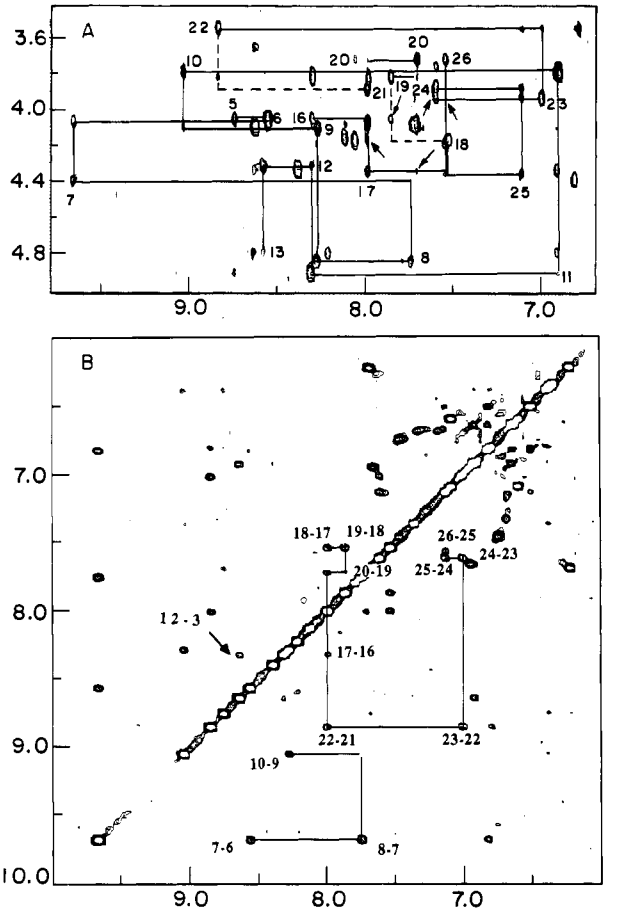


FIGURE 2: (A) "Fingerprint" region of the NOESY spectrum of ZFY-switch in $H_2O$; sequential $H_N$–$H_\alpha$ assignment is shown. Arrows indicate helix-related ($i$, $i + 3$) NOEs. (B) Portion of 2D NOESY spectrum of ZFY-switch showing NOEs between amide protons. Assignments are indicated along the axes. Arrow indicates $\beta$-sheet-related NOE between residues 3 and 12.

Table II: Differences in Chemical Shift Values[a] between ZFY-switch and ZFY-6

| | chemical shifts at 25 °C | | | |
|---|---|---|---|---|
| residue | NH | $C_\alpha H$ | $C_\beta H$ | others |
| 20 T | −0.35 | −0.1 | −0.1 | $C_\gamma H_3$ −0.1 |
| 21 H | −0.25 | −0.05 | −0.4, −0.1 | $C_2H$ −0.12; $C_4H$ −0.3 |
| 22 I | −0.2 | 0.1 | −, − | − |
| 23 K | −0.7 | −0.05 | −0.1, − | − |
| 24 T | −0.3 | −0.3 | 0.1 | $C_\gamma H_3$ −0.15 |
| 25 H | −0.25 | −0.7 | −0.3, − | − |

[a] Differences are given for those residues for which at least one proton exhibits a change in chemical shift of >±0.2 ppm (25 °C and pH 6.0) relative to the parent peptide (ZFY-6; Kochoyan et al., 1991a).

(Kochoyan et al., 1991a) and will not be described in detail. The fingerprint region of the NOESY spectrum of ZFY-switch, which contains sequential $d_{\alpha N}$ NOEs, is shown in Figure 2A; the amide region, which contains sequential $d_{NN}$ NOEs, is shown in Figure 2B. These spectral regions also contain NOEs characteristic of secondary structure: arrows indicate helix-related ($i$, $i + 3$) contacts in panel A and a $\beta$-strand-related $H_N$–$H_N$ contact (between residues 3 and 12) in panel B. Additional cross-strand contacts are observed between residues 2–13 and 4–11 (not shown).

The observed chemical shifts (Table I) are in general similar to those of ZFY-6. Differences (>0.2 ppm) are observed involving residues 20–25 (Table II); selected examples are illustrated in panels B and C of Figure 1. Interestingly, the histidine ring resonances ($H_\delta$ and $H_\epsilon$; labeled a–d in Figure

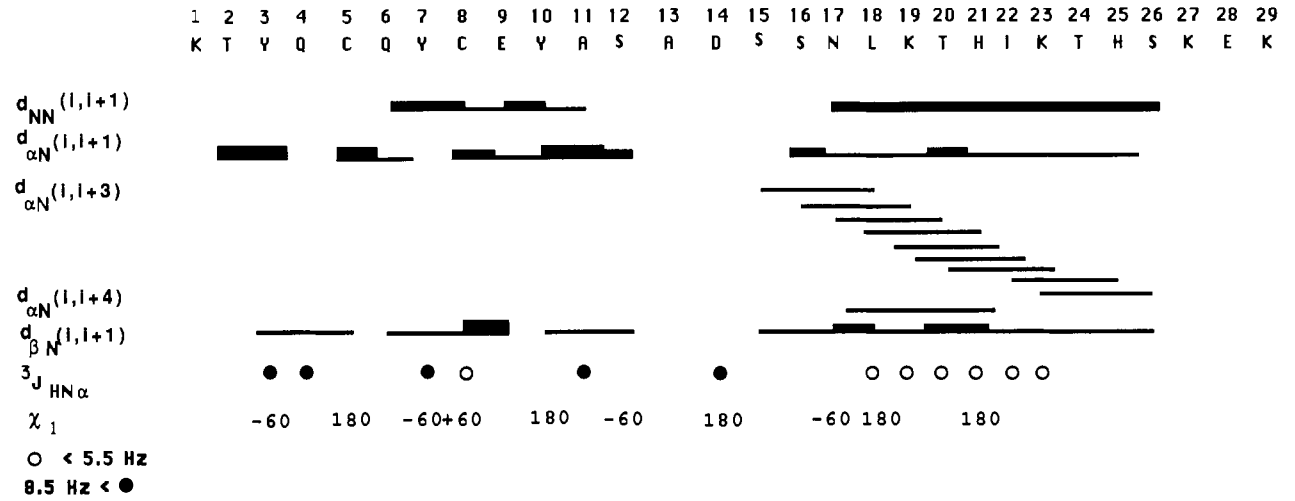


FIGURE 3: Summary of sequential connectivities, $^3J_{NH\alpha}$ coupling constants, and $\chi_1$ dihedral restraints in ZFY-switch. The observed pattern of NOEs and coupling constants is in general similar to that of the parent peptide (Kochoyan et al., 1991a); selected differences are observed involving residues 19–25. Chemical shifts are given in Table I.

1) exhibit essentially identical chemical shifts in the two spectra, suggesting a detailed correspondence of internal architecture in the two fingers. In each case histidine coordination occurs in a Zn–$H_\delta$ linkage, as indicated by strong $H_\delta$–$H_\delta$ NOE between H21 and H25 (H26 in ZFY-6) as discussed by Klevit et al. (1990). We note in passing that whereas the H26 $\beta$ resonances are resolved (and stereospecifically assigned) in the spectrum of ZFY-6 (Kochoyan et al., 1991a,b), the corresponding H25 $\beta$ resonances are unresolved in the spectrum of ZFY-switch (Table I). This ambiguity limits the local precision of the DG/RMD structures (see below).

Sequential and medium-range NOEs and selected coupling constants are shown in Figure 3 in the schematic form developed by Wuthrich (1986). The secondary structure of ZFY-switch, as inferred from the relationships shown in the figure, consits of an N-terminal $\beta$-hairpin (residues 2–13) and C-terminal helix (residues 15–26). This pattern (designated the $\beta\beta\alpha$ motif) is similar to that obtained for the parent peptide (Kochoyan et al., 1991a); however, local differences in NOE intensities and $^3J_{\alpha N}$ coupling constants are observed near the site of deletion. The structural implications of these differences are explored below. Long-range NOEs are observed involving the conserved framework residues C5, C8, Y10, L18, H21, and H25; these are also similar in those of ZFY-6 (Kochoyan et al., 1991a). With the exception of the Y10 side chain (see Materials and Methods), neither ZFY-6 nor ZFY-switch exhibits "doubling" of cross peaks, as observed in the spectrum of ADR1a (Xu et al., 1991).

*Solution Structure of ZFY-switch.* Twelve DG/RMD models were obtained on the basis of 171 NOE restraints; of these 67 were sequential, 41 were short range (between residues 2–4 positions apart in the sequence), and 63 were long range (>4 residues apart in the sequence). In addition, two intraresidue NOEs were used to restrain the configuration of the L18 side chain. *J* coupling constants were used to provide 12 $\phi$ and 10 $\chi_1$ restraints (Figure 3 and Table I). An analogous set of restraints was obtained for ZFY-6 (Kochoyan et al., 1991b), permitting meaningful comparison of the two structures. In one case (the C-terminal histidine), analogous restraints are less precise for ZFY-switch than for ZFY-6 due to degeneracy of the H25 $\beta$ resonances in the spectrum of the former (see above); in addition, whereas in ZFY-6 the large H26 $^3J_{HN\alpha}$ coupling (12 Hz) permitted inclusion of a dihedral restraint, in ZFY-switch the analogous H25 $^3J_{HN\alpha}$ coupling (7.5 Hz) cannot be interpreted unambiguously. A statistical

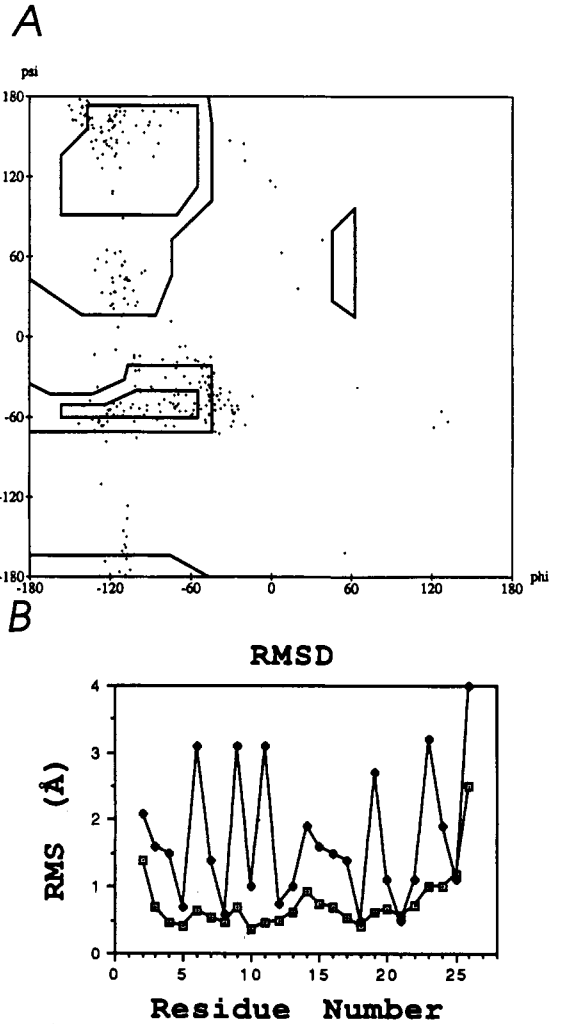


FIGURE 4: (A) Ramachandran plot for ZFY-switch ensemble (residues 2–26). (B) Summary of RMS deviations by residue: side-chain atoms (◆) and backbone atoms (□). These values are similar to those for the wild-type domain (Kochoyan et al., 1991b).

description of the DG/RMD ensemble is provided in Table III; ensemble averages are given of rms restraint violations, deviations from ideal covalent geometry, and the individual terms of the restrained empirical energy function. Figure 4A contains a Ramachandran plot of ($\phi$,$\psi$) dihedral angles;

Table III: ZFY-switch Statistical Parameters (Ensemble Averaged)

| | number | rms |
|---|---|---|
| NMR Restraint Violations[a] | | |
| NOEs | 171 | 0.011 Å |
| Deviation from Ideal Covalent Geometry[b] | | |
| bond lengths | 485 | 0.016 Å |
| bond angles | 874 | 2.6° |
| Empirical Energy Function[b,c] | | |
| total | | −2.3 |
| van der Waals | | −144.0 |
| hydrogen bonds | | −33.4 |
| improper dihedral angles | | 2.4 |
| constrained dihedral angles | | 0.76 |
| NOE constraint energy | | 0.8 |
| covalent bond lengths | | 5.8 |
| dihedral angles | | 77.8 |
| bond angles | | 86.0 |

[a] NOE restraint violations represent rms upper-bound violations; no lower bounds were assumed (see Materials and Methods). Dihedral angle restraint violations represent deviations greater than ±40°. [b] Empirical energies were calculated with the CHARMm potential energy function; the NOE force constant was 40 kcal/Å$^2$, and the dihedral force constant was 40 kcal/radian$^2$. [c] All values are given in kilocalories per mole.

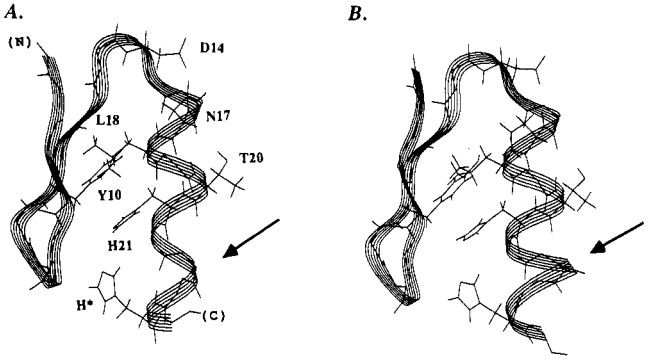


FIGURE 5: Ribbon representation of ZFY-switch (A) and ZFY-6 (B) showing positions of conserved cysteines and histidines (H21 and H*) involved in metal coordination, framework residues Y10 and L18, and putative DNA contact residues D14, N17, and T20. Site of deletion in ZFY-switch is indicated by an arrow. Rms deviations are given by residue in panel B of Figure 4. The precision with which the main chain is defined in the DG/RMD ensemble is illustrated in Figure 6A; the precision with which the side chains of residues C5, C8, Y10, L18, H21, and H* are defined is illustrated in Figure 6B.

backbone and side-chain rms deviations are shown by residue number in Figure 4B.

DG/RMD calculations demonstrate that ZFY-6 and ZFY-switch adopt similar overall three-dimensional structures, as illustrated by representative ribbon models in Figure 5. Arrows indicate local changes in backbone configuration at the site of deletion; these changes are described in detail below. An ensemble of backbone configurations of ZFY-switch (shown in red in Figure 6A) is essentially identical with that of ZFY-6 (shown in green in Figure 6A). Among unrelated Zn fingers only local differences are observed in the details of the $\beta$-sheet and in the loop associated with variant $HX_3H$, $HX_4H$, or $HX_5H$ ligand spacing (Figure 6C). Each finger exhibits a stably folded hydrophobic core involving analogous residues. In the case of ZFY-switch the following residues are well-order: Y3, C5, Y7, C8, Y10, S12, L18, T20, H21, I22, and H25 (side-chain rms deviations <1.2 Å; see Figure 4B). The positions of selected internal side chains are shown in Figure 5A (representative structure) and Figure 6B (ensemble). Residues presumed by analogy contact DNA bases (D14, N17, and T20; Pavletich & Pabo, 1991) are on the surface of both ZFY-6 and ZFY-switch (Figure 5). Residues 1 and 27–30 in ZFY-switch appear to be disordered in solution and are not considered further.

*Comparison of C-Terminal Helices.* In the 2D-NMR structure of ZFY-6 a distortion in $\alpha$-helical geometry was observed in association with the $HX_4H$ ligand spacing (Kochoyan et al., 1991a); this nonstandard loop makes possible two sets of bifurcating hydrogen bonds (between the amide proton of T24 and the carbonyl oxygens of T20 and H21 and between the carbonyl of H21 and the amide protons of T24 and K25; Kochoyan et al., 1991b). This nonstandard structure is not observed in ZFY-switch. Instead, in the majority of structures the C-terminal $\alpha$-helix continues between the histidines as a $3_{10}$ helix, as previously observed in a consensus $HX_3H$ finger (Xfin31; Lee et al., 1989).

The following hydrogen-bonding pattern is observed in the ZFY-switch ensemble. $\alpha$-Helical ($i$, $i+4$) hydrogen bonds are predicted in each DG/RMD structures from residues 15 to 18. The carbonyl oxygen of residue 19 does not consistently accept a hydrogen bond and separates $\alpha$- and $3_{10}$-segments. A $3_{10}$-related ($i$, $i+3$) hydrogen bond is observed in almost all structures between the carbonyl oxygen of residue 20 and the amide proton of residue 23. In the majority of structures, residues 21 and 22 exhibit similar ($i$, $i+3$) hydrogen bonds or bifurcated ($i$, $i+3$) and $\alpha$-helix-related ($i$, $i+4$) hydrogen bonds. These results are consistent with a higher resolution view provided by the crystal structure of a Zn finger–DNA complex (Zif268; Pavletich & Pabo, 1991). In this structure of C-terminal helix is separated into $\alpha$ and $3_{10}$ segments by a kink at residue 19 (present numbering scheme; Figure 1A). At the C-terminus the helix then extends by two residues into the linker (residues 26 and 27 in the present numbering scheme) with formation of two ($i$, $i+4$) $\alpha$-helical hydrogen bonds (22–26 and 23–27). In ZFY-switch the analogous 22–27 hydrogen bond is not observed as residue 27 is disordered.

Deletion of residue 25 in ZFY-switch thus results in a structural switch to an alternative hydrogen-bonding scheme and surface architecture. Evidently, the histidine-associated surfaces in ZFY-6 and ZFY-switch are locally encoded, i.e., these surfaces can be designed independently of the rest of the Zn finger sequence. In panel C of Figure 6 are shown representative $HX_3H$ [ZFY-switch (green) and Xfin31 (blue)], $HX_4H$ (red; Kochoyan et al., 1991b), and $HX_5H$ (yellow; Omichinski et al., 1990) domains. An alignment of corresponding C-terminal regions is shown in panel D. Among "ambiguous" Zn finger sequences containing more than one possible coordination scheme (e.g., $HX_3HXH$), ligand selection appears to be determined by the relative local stabilities of these alternative structures (Weiss et al., 1991).

## Discussion

The classical Zn finger motif ($CX_{2,4}CX_9LX_2HX_{3-5}H$) provides a structural mechanism to achieve a well-defined protein surface for macromolecular recognition. A majority of classical Zn finger sequences exhibit a single-finger repeat, suggesting a corresponding structural repeat in the protein–DNA complex (Fairall et al., 1986; Gibson et al., 1988; Berg, 1988, 1990). Such a repeat has recently been observed in an X-ray structure of a representative complex (Pavletich & Pabo, 1991); three successive CC/HH fingers bind in the major groove by an equivalent mechanism. It is not known whether this mechanism will extend to families of Zn finger proteins with second-order sequence repeats (Page et al., 1987; Nietfeld et al., 1989). These families exhibit systematic alternation between $HX_3H$- and $HX_4H$-containing domains whose func-

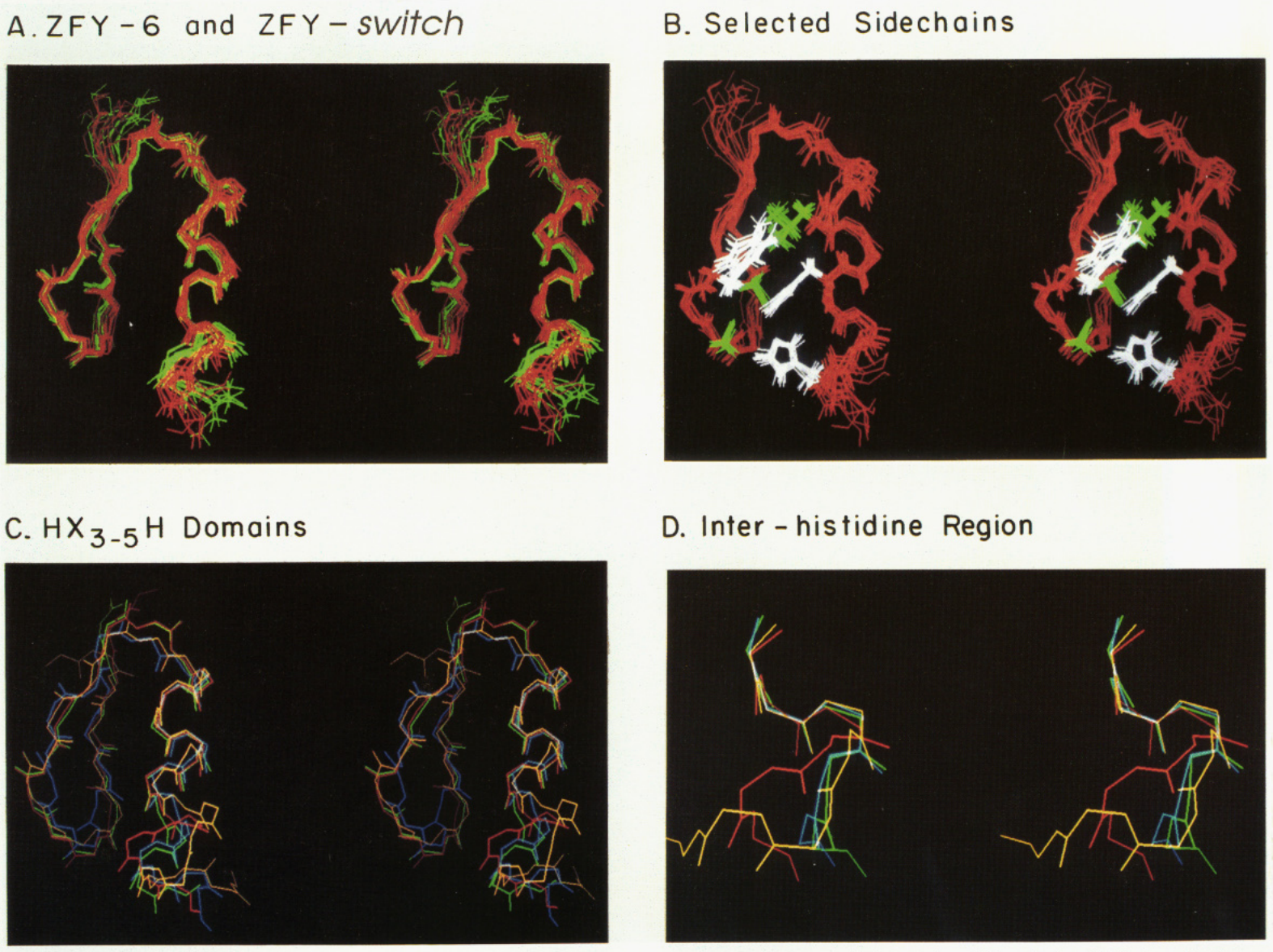


FIGURE 6: (A) Stereo representation of DG/RMD ensembles. The backbone structures of ZFY-6 are shown in green, and those of ZFY-switch are in red. A local difference is observed between the histidines (arrow). Each ensemble contain 12 structures; the two structures are aligned along the backbone atoms of residues 2–21. (B) Selected side chains in ZFY-switch (see Figure 5 for residue labels). For clarity, the side chains are shown in alternating colors (white/green) from bottom to top: C5 (bottom left in green) and H25 (bottom right in white); C8 (middle left in green) and H21 (middle right to white); Y10 (top left in white) and L18 (top right in green). (C) Alignment of representative $HX_{3-5}H$ Zn finger domains: $HX_5H$ (yellow; Omichinski et al., 1990), $HX_4H$ (red; Kochoyan et al., 1991b), $HX_3H$ (green, this study; blue, Lee et al., 1989). (D) Comparison of backbone configurations in the interhistidine regions of representative $HX_{3-5}H$ domains. The color scheme is the same as in panel C. The structures are aligned with respect to the N-terminal portion of the helix (residues 15–21 as numbered in Figure 1A).

tional implications are not presently understood. A model of the ZFY–DNA complex has been proposed (Kochoyan et al., 1991a,b) and analyzed in relation to model II of Klug and colleagues (Fairall et al., 1986; Churchill et al., 1990).

In this paper we have determined the 2D-NMR structure of a novel $HX_3H$ analogue (ZFY-switch) of a previously characterized $HX_4H$ Zn finger (ZFY-6; Kochoyan et al., 1991b). The parent and mutant peptides exhibit similar metal-dependent folding with tetrahedral coordination; optical pH titration of the $Co^{2+}$ complexes demonstrates that the thermodynamic stability of ZFY-switch is comparable to other ZFY-related Zn fingers (Weiss et al., 1990; Weiss & Keutmann, 1990). The tetrahedral metal-binding site and hydrophobic core of ZFY-switch, as visualized by DG/RMD reconstruction, are essentially identical to those of ZFY-6. Differences between the two structures are localized to the $HX_nH$ site. Whereas ZFY-6 contains a $HX_4H$-associated nonstandard loop, the variant $HX_3H$ site folds predominantly as a $3_{10}$ extension of the C-terminal $\alpha$-helix, as previously observed in the solution structure of Xfin-31 (Lee et al., 1989) and defined at higher resolution in the crystal structure of the Zif268–DNA complex (Pavletich & Pabo, 1991). Comparison of these and related structures (Klevit et al., 1990; Omichinski et al., 1990) demonstrates that variation in histidine spacing enables a surface of the Zn finger to be designed independently of the rest of the domain.

In the crystal structure of a representative Zn finger–DNA complex (Pavletich & Pabo, 1991) the canonical $HX_3H$ surface is oriented near the finger-linger exit from the major groove. In this structure the C-terminal helix extends two residues into the linker, forming in effect a turn that defines in part the relative orientation of successive fingers. In addition, the side chain of the central residue (position 23 in the present numbering scheme) contacts a backbone carbonyl oxygen of the successive finger. Each of these features would be altered in $HX_4H$ domains. The striking conservation of $HX_3H$ and $HX_4H$ domains in alternating Zn finger motifs suggests distinct functional roles for $HX_3H$- and $HX_4H$-associated hydrogen-bonding schemes and protein surfaces. In the future these roles may be defined by structural studies of alternating two-finger units.

## Acknowledgments

We thank K. A. Mason for technical assistance, J. Lee for assistance with NMR measurements, P. E. Wright and D. A. Case for coordinates (Xfin-31) and helpful discussion, G. M. Clore and A. Gronenborn ($HX_5H$ domain; Omichinski et al., 1990) and N. Pavletich and C. O. Pabo (Zif268) for respective coordinates, T. F. Havel for the program DG-II, and A. T. Brunger for XPLOR.

## Supplementary Material Available

One table listing metal-related, dihedral, and NOE restraints (4 pages). Ordering information is given on any current masthead page.

## References

Baldwin, A. S., LeClair, K. P., Singh, H., & Sharp, P. A. (1990) *Mol. Cell. Biol. 10*, 1406–1412.

Barany, G., & Merrifield, R. B. (1979) in *The Peptides* (Gross, E., & Meienhofer, J., Eds.) Vol. 2, pp 1–284, Academic Press, New York.

Berg, J. M. (1988) *Proc. Natl. Acad. Sci. U.S.A. 85*, 99–487.

Brooks, B. R., Bruccoleri, R. E., Olafson, B. O., States, D. J., Swaminathan, S., & Karplus, M. (1983) *J. Comput. Chem. 4*, 187–217.

Churchill, M. E. A., Tullius, D. T., & Klug, A. (1990) *Proc. Natl. Acad. Sci. U.S.A. 87*, 5528–5532.

Clore, G. M., Gronenborn, A. M., Brunger, A., & Karplus, M. (1985) *J. Mol. Biol. 186*, 435–455.

DiLella, A. G., Page, D. C., & Smith, R. G. (1990) *New. Biol. 2*, 49–55.

Fairall, L., Rhodes, D., & Klug, A. (1986) *J. Mol. Biol. 192*, 577–591.

Frankel, A. D., Berg, J. M., & Pabo, C. O. (1987) *Proc. Natl. Acad. Sci. U.S.A. 84*, 4841–4845.

Gibson, T. J., Postma, J. P. M., Brown, R. S., & Argos, P. (1988) *Protein Eng. 2*, 209–218.

Klevit, R. E., Herriott, J. R., & Horvath, S. (1990) *Proteins: Struct., Funct., Genet. 7*, 214–226.

Klug, A., & Rhodes, D. (1987) *Trends Biochem. Sci. 12*, 464–468.

Kochoyan, M., Havel, T. F., Nguyen, D., Dahl, C. E., Keutmann, H. T., & Weiss, M. A. (1991a) *Biochemistry 30*, 3371–3386.

Kochoyan, M., Keutmann, H. T., & Weiss, M. A. (1991b) *Biochemistry 30*, 7063–7072.

Koopman, P., Gubbay, J., Colignon, J., & Lovell-Badge, R. (1989) *Nature 342*, 940–942.

Lee, M. S., Gippert, G. P., Soman, K. V., Case, D. A., & Wright, P. E. (1989) *Science 245*, 635–637.

Maekawa, T., Sakura, G., Sudo, T., & Ishii, S. (1989) *J. Biol. Chem. 264*, 14591–14595.

Nietfeld, W., El-Baradi, T., Mentzel, H., Pieler, T., Koster, M., Poting, A., & Knochel, W. (1989) *J. Mol. Biol. 208*, 639–659.

Omichinski, J. G., Clore, G. M., Apella, E., Sakaguchi, K., & Gronenborn, A. M. (1990) *Biochemistry 29*, 9324–9334.

Page, D. C., Mosher, R., Simpson, E., Fisher, E. M. C., Mardon, G., Pollack, J., McGillivray, B., de la Chapelle, A., & Brown, L. G. (1987) *Cell 51*, 1091–1104.

Page, D. C., Fisher, E. M. C., McGillivrany, B., & Brown, L. G. (1990) *Nature 346*, 279–281.

Palmer, M. S., Sinclair, A. H., Berta, P., Ellis, N. A., Goodfellow, P. N., Abbas, N. E., & Fellous, M. (1989) *Nature 342*, 937–939.

Parraga, G., Horvath, S. J., Eisen, A., Taylor, W. E., Hood, L., Young, E. T., & Klevit, R. E. (1988) *Science 241*, 1489–1492.

Parraga, G., Horvath, S., Hood, L., Young, E. T., & Klevit, R. E. (1990) *Proc. Natl. Acad. Sci. U.S.A. 87*, 137–141.

Pavletich, N. P., & Pabo, C. O. (1991) *Science 252*, 809–817.

Stewart, J. M., & Young, J. D. (1984) *Solid Phase Peptide Synthesis*, Raven Press, New York.

Tregear, G. W., van Reitschoten, J., Sauer, R. T., Niall, H. D., Keutmann, H. T., & Potts, J. T. (1977) *Biochemistry 16*, 2817–2823.

Weiss, M. A., & Keutmann, H. T. (1990) *Biochemistry 29*, 9808–9813.

Weiss, M. A., Mason, K. A., Dahl, C. E., & Keutmann, H. T. (1990) *Biochemistry* 29, 5560–5664.

Weiss, M. A., Markus, M. A., Biancalana, S., Dahl, C. E., Keutmann, H. T., & Hudson, D. (1991) *J. Am. Chem. Soc. 113*, 6704–6706.

Wuthrich, K. (1986) *NMR of Proteins and Nucleic Acids*, Wiley, New York.

Xu, R. X., Horvath, S. J., & Klevit, R. E. (1991) *Biochemistry 30*, 3365–3371.